EPHB4 kinase inactivating mutations cause autosomal dominant lymphatic-related hydrops fetalis

Silvia Martin-Almedina,[1*] Ines Martinez-Corral,[2*] Rita Holdhus,[3] Andres Vicente,[4] Elisavet Fotiou,[1] Shin Lin,[5,6] Kjell Petersen,[7] Michael A Simpson,[8] Alexander Hoischen,[3,9] Christian Gilissen,[9] Heather Jeffery,[1] Giles Atton,[10] Christina Karapouliou,[1] Glen Brice,[10] Kristiana Gordon,[11] John W Wiseman,[12] Marianne Wedin,[12] Stanley G Rockson,[5] Steve Jeffery,[1] Peter S Mortimer,[1] Michael P Snyder,[6] Siren Berland,[13] Sahar Mansour,[10] Taija Makinen,[2] Pia Ostergaard[1]

[1]Lymphovascular Research Unit, Cardiovascular and Cell Sciences Institute, St George's University of London, London, UK

[2]Department of Immunology, Genetics and Pathology, Uppsala University, Uppsala, Sweden.

[3]Genomics Core Facility, Department of Clinical Science, University of Bergen, Norway.

[4]Lymphatic Development Laboratory, Cancer Research UK London Research Institute, London, UK.

[5]Division of Cardiovascular Medicine, Stanford University, Stanford, California, USA

[6]Department of Genetics, Stanford University, Stanford, California, USA

[7]Computational Biology Unit, Department of Informatics, University of Bergen, Norway

[8]Division of Genetics and Molecular Medicine, Kings College London School of Medicine, Guy's Hospital, London, UK

[9]Department of Human Genetics, Radboud University Medical Center and Donders Centre for Neuroscience, Radboud University Medical Center, Nijmegen, The Netherlands

[10]South West Thames Regional Genetics Unit, St George's University of London, London, UK

[11]Department of Dermatology, St George's University Hospital NHS Foundation Trust, London, UK

[12]Discovery Sciences, RAD-Transgenics, AstraZeneca R&D, Mölndal, Sweden

[13]Center for Medical Genetics and Molecular Medicine, Haukeland University Hospital, Bergen, Norway

* Authorship note: Silvia Martin-Almedina and Ines Martinez-Corral contributed equally to this work.

The authors have declared that no conflict of interest exists.

Corresponding author: Pia Ostergaard, Lymphovascular Research Unit, Cardiovascular & Cell Sciences Institute, St George's University of London, Cranmer Terrace, London SW17 0RE, UK. Phone +44 (0)208 725 0192; Email: posterga@sgul.ac.uk

Abstract

Hydrops fetalis describes fluid accumulation in at least 2 fetal compartments, including abdominal cavities, pleura, and pericardium, or in body tissue. The majority of hydrops fetalis cases are nonimmune conditions that present with generalized edema of the fetus, and approximately 15% of these nonimmune cases result from a lymphatic abnormality. Here, we have identified an autosomal dominant, inherited form of lymphatic-related (nonimmune) hydrops fetalis (LRHF). Independent exome sequencing projects on 2 families with a history of in utero and neonatal deaths associated with nonimmune hydrops fetalis uncovered 2 heterozygous missense variants in the gene encoding Eph receptor B4 (EPHB4). Biochemical analysis determined that the mutant EPHB4 proteins are devoid of tyrosine kinase activity, indicating that loss of EPHB4 signaling contributes to LRHF pathogenesis. Further, inactivation of Ephb4 in lymphatic endothelial cells of developing mouse embryos led to defective lymphovenous valve formation and consequent subcutaneous edema. Together, these findings identify EPHB4 as a critical regulator of early lymphatic vascular development and demonstrate that mutations in the gene can cause an autosomal dominant form of LRHF that is associated with a high mortality rate.

Introduction

Hydrops fetalis decribesis defined as excessive fluid accumulation or edema in at least two fetal compartments. Non-immune hydrops fetalis is the cause in more than 85% of cases, of which 15% have been reported to have a lymphatic related abnormality (1). In 20% of non-immune hydrops fetalis cases the cause is not known. Lymphatic-related (non-immune) hydrops fetalis (LRHF) has been included in a subgroup of primary lymphedemas under the umbrella term Generalised Lymphatic Dysplasia (GLD) by Connell *et al*. (2). In this classification, GLD was defined as lymphedema associated with systemic or visceral involvement (including hydrops fetalis), even if the lymphedema was not widespread. The GLD group includes patients with a widespread developmental abnormality of the lymphatic system, often presenting prenatally with hydrothoraces or non-immune hydrops fetalis.

Hennekam syndrome (OMIM#235510) is an example of a GLD which is inherited in an autosomal recessive manner. Mutations in collagen and calcium binding EGF domain 1 (*CCBE1)* and FAT atypical cadherin 4 (*FAT4)* have been identified as causal (3-5). Another recessively inherited form of GLD with a high incidence of LRHF has recently been reported as caused by mutations in piezo-type mechanosensitive ion channel component 1 (*PIEZO1)* (6), adding to the genetic heterogeneity of the GLD group.

We have recently ascertained two families with a history of non-immune hydrops and postnatal lymphatic dysfunction, but with a pattern suggestive of autosomal dominant inheritance, and with sporadic occurrence in one of the families. We have identified heterozygous inactivating mutations in the kinase domain of *EPHB4* as causative for this condition. This suggests not only is LRHF/GLD genetically heterogeneous, but it should also be considered in both dominant and recessive forms. The importance of Ephb4 for

lymphatic vascular development is further supported by analysis of a genetic mouse model with lymphatic endothelial specific deletion of *Ephb4*.

Results

Genetic analysis of LRHF identifies causative mutations in EPHB4. We report two multigenerational families (one from Norway, GLD_{NOR}, and one from the UK, GLD_{UK}) (Figure 1). Clinical findings in these families include antenatal non-immune hydrops fetalis or bilateral hydrothoraces, and neonatal chylothoraces of variable severity (Table 1) and a high number of first trimester miscarriages (GLD_{NOR}). The non-immune hydrops fetalis is associated with a high mortality, but babies surviving the neonatal period improve with time, with spontaneous resolution of the hydrops and pleural effusions. Only one (GLD_{UK}:I.2) of five adults has developed peripheral edema of the lower extremities in adolescence (Figure 2) but three of the five adults (GLD_{NOR}:II.2, GLD_{NOR}:II.3 and GLD_{UK}:I.2) have varicose veins. Although GLD_{UK}:II.2 and GLD_{NOR}:II.2 currently have no clinical evidence of peripheral lymphedema, lymphoscintigraphy showed mild bilateral impairment of lymph drainage with retention of tracer in the lower limbs in both. In addition, GLD_{UK}:II.2 had an atrial septal defect, diaphragmatic hernia and cystic hygroma at birth. There appears to be an association with atrial septal defect (ASD) in both families (n=7).

Sanger sequencing identified no pathogenic variants in the genes known to be associated with congenital primary lymphedema (i.e. *CCBE1, VEGFR3* and *VEGFC*) in the UK proband (GLD_{UK}:I.2). Whole-exome sequencing (WES) was performed on the family to identify pathogenic variants. When filtering the WES data of the UK family for variants in genes known to have relevance to the lymphatic system and lymphangiogenesis, an unreported variant (NM_004444.4: c.2216G>A, p.Arg739Glu) in *EPHB4* was identified. Initially, it was thought that the variant did not fully co-segregate with the disorder status in the family (Figure 1A), as two clinically unaffected family members were found to carry the variant

(GLD_{UK}:II.4 and GLD_{UK}:III.2). Neither of these presented with hydrops fetalis but both were later diagnosed with an ASD. The next step of the analysis was to apply a specific autosomal dominant inheritance filter criterion and *MIER2* was the only gene that fulfilled that (Figure 1A). However, the *MIER2* variant (NM_017550.1: c.865C>T, p.Arg289Trp) has been reported as a SNP (rs148482834) with a heterozygous genotype observed at a frequency of 0.001.

Meanwhile, an independent study of a Norwegian GLD family was undertaken. In this family, the condition initially appeared to be sporadic in monozygotic twins (GLD_{NOR}:II.2 and II.3), who both had subcutaneous edema at birth that resolved in infancy (Table 1). GLD_{NOR}:II.3 required ventilation and thoracentesis for bilateral chylothoraces. Both sisters had sons with non-immune hydrops, one died at 1.5 days of age, the other was moribund in the neonatal period but the edema eventually resolved. Both sons also had an ASD. Three genes (*PTPN11, FOXC2* and *VEGFR3*) were ruled out in GLD_{NOR}:II.2 by Sanger Sequencing, and a high resolution microarray CGH (Affymetrix 6.0) was normal in GLD_{NOR}:II.3. When analysing the WES data, the only gene to fulfil an autosomal dominant model with *de novo* occurrence was *EPHB4*. Sanger sequencing of additional family members showed all affected family members to carry the variant (c.2345T>G, p.Ile782Ser) (Figure 1B). GLD_{NOR}:II.2 and II.3 were bout found to be mosaic for this variant and GLD_{NOR}:II.2 had a lower mutation load than her twin sister, GLD_{NOR}:II.3, consistent with her milder neonatal presentation (Supplemental Figure 1).

As *MIER2* had shown perfect co-segregation in $GLD_{UK,}$ the WES data of GLD_{NOR}:III.5 was scrutinised but no variants were found in *MIER2* and the coverage was found to be of sufficient depth and quality. For good measure, GLD_{NOR}:III.5 was also screened by Sanger sequencing for all exons of *MIER2*; still no variant was identified. Neither *EPHB4* variants had

been previously reported in public databases or in 900 in-house controls and it was therefore concluded that mutations in *EPHB4* are the likely cause of the LRHF/GLD phenotype seen in these two families despite the variable expression observed.

LRHF associated mutations lead to inactive EPHB4 kinase. EPHB4 binds the transmembrane ephrinB2. Binding of ephrinB2 to EPHB4 stimulates phosphorylation and activates downstream signalling cascades (7, 8). The two *EPHB4* mutations (p.Arg739Glu and p.Ile782Ser) occur at highly conserved residues located in the tyrosine kinase domain of the EPHB4 protein (Supplemental Figure 2 and 3A). Moreover, p.Arg739Glu is located within the catalytic loop HRD (His-Arg-Asp) motif, also highly conserved in many tyrosine kinases (Supplemental Figure 3B). To investigate the effect of the mutations identified in the patients with LRHF, corresponding expression constructs for wild-type (WT) and mutant proteins by site-directed mutagenesis were generated and analysed for their phosphorylation activity after transient transfection in HEK293T cells. The tyrosine phosphorylation levels of WT, p.Arg739Glu and p.Ile782Ser mutants were analysed by immunoprecipitation and western blotting with anti-EPHB4 and anti-phosphotyrosine specific antibodies. Mutant proteins showed no phosphorylation (Figure 3A), suggesting that both mutations alter EPHB4 signalling in patients with LRHF/GLD. To test the possibility that the mutations were interfering with the phosphorylation state of the WT protein, different ratios of WT and mutant proteins were co-transfected and phosphorylation of the receptor analysed as described above. Results showed no dominant negative effect, as phosphorylation of the total receptor decreased when increasing amounts of mutated receptor were co-transfected (Figure 3B). Furthermore, EphrinB2-dependent EPHB4 activation was evaluated in lymphatic endothelial cells (LECs) after expression of Myc-DDK

tagged EPHB4. To distinguish phosphorylation levels of Myc-DDK tagged exogenous expressed WT and mutant EPHB4 from endogenous expressed WT EPHB4, an anti DDK antibody was used for the immunoprecipitation and isolation of only the overexpressed forms of Myc-DDK tagged EPHB4. EphrinB2 treatment increased phosphorylation level of WT Myc-DDK tagged EPHB4 but not mutant proteins (Figure 4), confirming the negative effect of both mutations on the receptor activity after ligand stimulation in LECs.

Ephb4 deficiency in mice results in subcutaneous edema and abnormal lymphatic development. EphrinB2 -EphB4 signalling is critically required for the development of the cardiovascular system during early embryogenesis (9, 10). EphrinB2 and EphB4 are also essential for lymphatic vessel remodelling and valve formation during late embryonic and early postnatal development (11, 12), but whether they have an earlier role in lymphatic vessel morphogenesis that could explain *Ephb4* loss of function induced LRHF/GLD in humans is not known. Whole mount immunofluorescence analysis confirmed the previously reported venous and lymphatic endothelial specific expression of EphB4 in embryonic skin and mesenteries (Supplemental Figure 4A and B). To assess the potential contribution of lymphatic endothelial loss of EphB4 function to LRHF/GLD, we deleted *Ephb4* specifically in the lymphatic vasculature using tamoxifen inducible *Prox1-CreER*^{T2} mice crossed with a conditional *Ephb4*^{flox} line (Figure 5A, Supplemental Figure 5). The mice were further crossed with the *R26-mTmG* double reporter to monitor Cre activity, and to label gene-deleted cells with green fluorescent protein (GFP). *Ephb4* deletion was induced from the earliest stage of lymphatic development by administration of 4-hydroxytamoxifen (4-OHT) for five consecutive days starting at E10.5 (Figure 5A). At E15.5 a high proportion of mutant embryos showed subcutaneous edema (Figure 5B, and Figure 5C, left panel). In addition, a

proportion of dermal lymphatic vessels contained blood in 71% of edematous mutant embryos (n=14), but not in non-edematous mutants (n=5) or in control embryos (n=20) (Figure 5C and data not shown). Whole-mount immunofluorescence of the skin revealed tortuous and dilated dermal lymphatic vessels in the *Ephb4* mutants (Figure 5C, right panels). Notably, abnormal vessel morphology was also observed in vessels that showed a low contribution of GFP^+ (i.e. *Ephb4* deficient cells) (Figure 5C), suggesting that edema and/or blood filling of lymphatic vessels secondarily caused vessel dilation. In support of a non-cell-autonomous effect of early embryonic deletion of *Ephb4* to dermal lymphatic vasculature, inactivation of *Ephb4* from E12.5, when dermal lymphatic vessel formation begins (13) (Figure 5A), resulted in normal vasculature despite efficient gene targeting (Figure 5D). These results suggest E10-E12 as a critical time-window for EphB4 function during lymphatic development.

Ephb4 is required for the formation of lymphovenous and lymphatic valves. Previous studies have shown that between E10.5-E13.5 formation of specialized lymphovenous valves (LVV) occurs at the connection sites between the primordial thoracic duct (pTD) and the cardinal vein (14-16) (Figure 6A). It was therefore reasoned that edema in *Ephb4* mutants might be due to defective LVVs leading to inefficient lymph drainage. To investigate this, we induced Cre recombination in the developing LVVs in *Ephb4^{flox};R26-mTmG;Prox1-CreER^{T2}* embryos by 4-OHT treatment between E10.5-E12.5. Analysis of immunostained transverse vibratome sections of E13.5 control embryos showed preferential and efficient targeting of the dual LVVs by the *Prox1-CreER^{T2}* transgene, while pTD endothelium exhibited mosaic labeling (Figure 6B). Control LVVs (11 out of 11) consisted of two well-defined leaflets extending to the lumen of the cardinal vein (Figure 6C and 6D, Supplemental Movie 1). In contrast, the

majority of Ephb4 deficient LVVs (9 out of 13) did not show extended leaflets but instead consisted of abnormal clusters of GFP^+ cells (Figure 6C and 6D, Supplemental Movie 2).

Interestingly, studies using a function blocking antibody and a chemical genetic approach showed that EphB4 kinase signalling regulates lymphatic valve formation (11), while genetic studies have demonstrated an important function for its ligand EphrinB2 in the formation of both lymphatic and venous valves (12, 17). Using our genetic loss-of-function model we confirmed the essential role of EphB4 in lymphatic valve morphogenesis. Deletion of *Ephb4* during embryonic valve formation led to a complete absence of valves that form in control mesenteries by E18.5 by lymphatic endothelial cells (LECs) expressing high levels of Prox1 (Supplemental Figure 4C). In addition, early postnatal deletion of *Ephb4* led to a complete loss of lymphatic valves (Supplemental Figure 4D). These results demonstrate a critical role of *Ephb4* in the formation and early postnatal maintenance of lymphatic valves, and highlight conserved mechanisms regulating the formation of valves at different anatomical sites.

Discussion

This study identifies the EPHB4 receptor tyrosine kinase as a critical regulator of early lymphatic vessel development and a novel causative gene for LRHF and primary lymphedema. We have shown here that kinase inactivating mutations in *EPHB4* can produce a lymphatic phenotype in humans that can be classified as LRHF/GLD. However, this phenotype shows highly variable expression. Some individuals present with severe *in utero* swelling, which may cause perinatal demise (or fully resolve to become completely asymptomatic), others with no edema but only an atrial septal defect. It can be distinguished from the majority of Hennekam Syndrome cases, where the swelling presents in the antenatal period but persists throughout life (3-5). The large number of miscarriages in GLD_{NOR} may well be related to this disorder. In this regard, it is of interest that EphB4 and ephrin-B2 have been shown to be instrumental in the human placental development (18). Invasive cytotrophoblasts uses the EPHB4 expression on veins to ensure that migration of these cells into EPHB4 expressing uterine veins is limited and instead biased toward the arterial side of the circulation (19). Expression of EPHB4 at half the levels normally encountered may disturb the complex migration patterns seen in the process of placentation. A failure of the invasive cytotrophoblasts to take on an arterial phenotype is suspected to lead to the loss of pregnancy during the late first or early second trimester (19). Perinatal deaths were also of a higher frequency in the autosomal recessive form of LRHF/GLD caused by *PIEZO1* mutations but, in this condition, were probably related to the hydrops fetalis (6).

Two GLD_{UK} family members (GLD_{UK}:II.4 and her son, GLD_{UK}:III.2) carry the variant but have no clinical history of pre- or postnatal swelling. On lymphoscintigraphy (GLD_{UK}:II.4),

quantification shows entirely normal levels of transport of lymph within the legs, but imaging is suggestive of rerouting through skin and superficial tissues rather than a main lymphatic tract as seen in the control (Figure 2B). She has a small ASD and interestingly her son had large, multiple ASDs requiring surgical closure. Variable expression has been observed in other primary lymphedemas e.g. PIEZO1-related LRHF/GLD (6).

Like other forms of GLD (4, 6), this novel condition presents antenatally with non-immune hydrops or pleural effusions. The swelling may completely resolve with no residual lymphatic phenotype, similar to observations in the recently identified *PIEZO1* related GLD (6). However, the report of one affected individual with bilateral lower limb edema (GLD_{UK}:I.2) with abnormal lymph scans suggests that there may be residual, lymphatic weakness in the survivors. Further studies will be needed to investigate the specific nature and extent of the lymphatic dysfunction in these patients.

LEC specific deletion of *Ephb4* in mouse embryos led to subcutaneous edema and abnormal lymphatic vessel morphology, thus recapitulating aspects of the human LRHF phenotype. Temporal analysis of Ephb4 function demonstrated a critical requirement of Ephb4 during early stages of lymphatic development. Specifically, we found that Ephb4 regulates the formation of lymphovenous valves that are critical for efficient lymphatic function by maintaining unidirectional flow of lymph into blood (14, 20, 21). We additionally confirmed the previously reported critical role of Ephb4 in both formation and maintenance of lymphatic valves (11). Lymphatic valve defects are, however, an unlikely cause of *in utero* swelling due to their late embryonic development (22, 23). We postulate, therefore, that defective lymphovenous valve formation, caused by the lack of EPHB4 could contribute to the LRHF seen in the GLD_{NOR} and GLD_{UK} patients. In agreement with this, defective LVVs

were recently demonstrated in mouse models of primary lymphedemas caused by loss of function of Foxc2, Connexin37 and Gata2 (16, 24).

Edema in the mouse embryos lacking Ephb4 specifically in the lymphatic endothelia appears to be milder than that observed in the patients, suggesting that defective lymphovenous valves may only partially explain human LRHF/GLD. It is well known that EphB4 is also expressed in venous and capillary endothelium (9, 10), and therefore the impact of the mutations on the venous system needs to be considered. In accordance with this hypothesis some of the patients (GLD_{NOR}:II.2 and II.3; GLD_{UK}:I.2) showed varicose veins, which would be consistent with a valve defect in the venous system and would support the contribution of vascular deficiency to the observed phenotype. Together with the varicose veins, the ASD observed in the patients could also be an important part of this phenotype. Both have been reported in Lymphedema Distichiasis Syndrome with a frequency of approximately 7% (ASDs) (25) and 100% (varicose veins) (26).

Kinase activity is critical for EphB4 forward signalling in lymphatic endothelia (11). Our in vitro data show that *EPHB4* mutants carrying the LRHF associated mutations p.Arg739Glu and p.Ile782Ser are kinase-dead but do not have a dominant negative effect on WT protein. In contrast, *VEGFR3* mutants in Milroy Disease have a slower turnover (27), which may affect the signalling capacity of the WT tyrosine kinase receptor due to accumulation of mutant receptors on the cell surface. Unlike typical receptor tyrosine kinases that dimerise upon ligand stimulation, Ephrin receptors form higher order clusters, with cluster size being an important determinant of the quality and strength of cellular response (28, 29). Inclusion of a kinase-dead receptor may thus significantly weaken the signalling strength of higher order clusters and thereby alter cellular responses. EphB2 receptor-mediated endocytosis

requires the kinase activity of the receptor (30), so that kinase-dead EphB4 could also show defective endocytosis, influencing clustering dynamics and cellular responses. Further studies will aim to investigate those and other functional consequences of the LRHF/GLD associated mutations.

In conclusion, we report on kinase inactivating *EPHB4* mutations in eleven individuals from two extended family pedigrees presenting with a phenotypic spectrum from severe, lethal non-immune hydrops to ASD only. The inheritance pattern is typical of autosomal dominant inheritance with variable expression. Using a genetic mouse model, we have further shown that *Ephb4* deficiency in lymphatic endothelium leads to defective lymphovenous valves, which may critically contribute to edema formation in LRHF/GLD patients. This is the first report in the literature of a human phenotype associated with *EPHB4* mutations and also the first report of an autosomal dominant form of LRHF.

Methods

Exome sequencing. For GLD_{UK}, sequencing libraries were made following the protocol from Roche/Nimblegen's SeqCap EZ Exome Library v2.0 kit. The libraries were then sequenced on HiSeq2000 (Illumina) machines. Sequence reads were aligned to the reference genome (hg19) using Novoalign (Novocraft Technologies). Duplicate reads, resulting from PCR clonality or optical duplicates, and reads mapping to multiple locations were excluded from downstream analysis. Depth and breadth of sequence coverage were calculated with custom scripts and the BedTools package (31).

All variants were annotated using a custom annotation pipeline. Single-nucleotide substitutions and small indel variants were identified and quality filtered within the SamTools software package (32) and in-house software tools (33). Variants were annotated with respect to genes and transcripts with the Annovar tool (34). Variants were filtered for novelty by comparing them to dbSNP135 and 1000 Genomes SNP calls and to variants identified in 900 control exomes (primarily of European origin), which were sequenced and analyzed by the same method. Summary statistics for the exome sequencing is given in Supplemental Tables 1 and 2. Analysis of the exome-variant profiles was performed under a model of a rare autosomal-dominant disorder; this model required one previously unobserved heterozygous variant for all affected individuals.

For GLD_{NOR} the sequencing analysis was performed using the SOLID 5500xl platform (Life Technologies). Exon sequences were enriched by SureSelect Human All Exon v5 (Agilent Technologies), which targets ~21,500 human genes, covering a total of 50Mb of genomic sequence. Read alignment and variant calling were performed with Lifescope v1.3 software. All variants were annotated using a custom annotation pipeline. Variants from the exome

were filtered for known variants in dbSNP, intronic and UTR variants, synonymous variants and variants in our in-house database. Variants with less than 5 variation reads were also omitted. Summary statistics for the exome sequencing is given in Supplemental Table 3.

Confirmation Sequencing. Samples of available family members were analyzed by Sanger Sequencing. Primers were designed for the coding regions and associated splice sites for exons 13 and 14 of *EPHB4* and all exons of *MIER2* using Primer3 software (35) or ExonPrimer (helmholtz-muenchen.de). Primer sequences listed in Supplemental Table 4. PCR products were sequenced using BigDye Terminator v1.1 and v3.1 chemistry (Life Technologies) and an ABI3130xla Genetic Analyser or 3730 DNA analyser (Life Technologies). Sequencing traces were visually inspected in Finch TV v1.4 (Geospiza Inc) and SeqScape® Software v2.5 (Life Technologies).

The twins in GLD_{NOR} were also examined for mosaicism, by Sanger sequencing on DNA extracted directly from blood (new sample), urine, saliva, and skin biopsy (fibroblasts).

The variants from the 2 families have been submitted to the Leiden Open Variation Database ($LOVD^3$) (genomic variants 0000095140 [c.2216G>A; p.(Arg739Gln)] and 0000095141 [c.2345T>G; p.(Ile782Ser)]; http://databases.lovd.nl/shared/genes/EPHB4).

Site-directed mutagenesis of EPHB4 constructs. The human EPHB4 mammalian expression plasmids pCMV6-XL6-EPHB4 (SC117357) and Myc-DDK-tagged pCMV6-Entry-EPHB4 (RC208559) were obtained from OriGene and used as templates for site-directed mutagenesis using the QuikChange II XL Site-Directed Mutagenesis Kit (Agilent). All primers were designed using QuikChange Primer Design (Agilent) and are listed in Supplemental Table 5. All constructs were verified by DNA sequencing.

Cell culture and transfection. HEK293T cells (kindly provided by Dr Tris McKay, St George's University of London, UK) were maintained in DMEM supplemented with 10% FBS. Transfection of HEK293T cells was performed with GeneJuice transfection reagent (Merk) following the manufacturer's protocol. $6x10^5$ cells/well were seeded in 6-well plates the day before transfection, and then they were transfected with 3 µl GeneJuice and 1 µg of DNA. Human dermal lymphatic endothelial cells (C-12217) were obtained from Promocell and maintained in supplemented endothelial cell growth medium MV2 (C-22022, Promocell) containing recombinant human VEGF-C (2179-VC-025, R&D systems). Transfection of LECs was performed with Viromer YELLOW (VY-01LB-01, Lipocalyx) following the manufacturer's recommendations. $2x10^5$ cells/well were seeded in fibronectin (F1141, Sigma)-coated 6-well plates the day before transfection and then transfected with 1 µg of DNA. For both cell types, lysates were collected 24 hours post-transfection and subjected to immunoprecipitation and western blot analysis.

Ligand activation of EPHB4 receptor. EphrinB2/Fc (7397-EB-050, R&D systems) or Fc fragment alone (CSB-NP005401h, Stratech) were clustered by incubation with a goat anti-human IgG Fc antibody (40C-CR2022G-FIT, Stratech) at a 1:2 ratio for 1 hour at 4°C. 18 hours post-transfection LECs were serum-starved for 6 hours and then treated with 1µg/ml clustered EphrinB2/Fc or Fc alone for 30 minutes before cell lysates collection.

Immunoprecipitation and western blot analysis. For immunoprecipitation of overexpressed WT and mutant EPHB4, transfected cells were harvested in 100 µl of lysis buffer (20 mM Tris pH 7.5, 150 mM NaCl, 0.5%Triton X-100) supplemented with protease and phosphatase inhibitors (Sigma). After clarification by centrifugation, 100 µg of total HEK293T cells protein lysate was incubated with 0.8 µg of goat anti-human EPHB4 antibody (AF3038, R&D

systems) overnight at 4°C. After incubation with protein A sepharose beads (Sigma) for 4 hours at 4°C, immune complexes were precipitated by centrifugation. 100 µl of total LECs protein lysate was incubated with 4 µg of mouse anti-DDK antibody (clone OTI4C5, TA50011, Origene) overnight at 4°C and immune complexes precipitated with protein G sepharose beads (Sigma). Immunoprecipitates were separated by SDS-PAGE and transferred to PVDF membranes. Immunoblot analysis was performed with goat anti-human EPHB4 (AF3038, R&D Systems) and mouse anti-phosphotyrosine (clone 4G10, 05-321, Millipore) antibodies. All uncropped western blots are shown in Supplemental Figures 6 and 7.

Mouse lines. R26-mTmG mice were acquired from the Jackson Laboratory (36). *Prox1-CreER*^{T2} mice were previously described (17). For the generation of the *Ephb4*^{flox} line, a conditional knock-out strategy, flanking *Ephb4* exons 2 and 3 with *LoxP* sites, was used to target the *Ephb4* locus. The targeting vector was built using homologous recombination in bacteria (37). A C57BL/6 mouse BAC, served as template for the extraction of the homology arms of the targeting vector. The targeting vector contained a *frt* flanked neomycin phosphotransferase, Neo, selectable marker cassette. After linearization, the targeting construct was electroporated into AZX1, a C57Bl/6JOlaHsd derived embryonic stem cell line. PCR screens and Southern blot analyses revealed clones that had undergone the desired homologous recombination event. Several of these clones were expanded and injected into Balb/cOlaHsd blastocysts to generate chimeric males which were then bred to C57Bl/6JOlaHsd females and black-coated offspring were genotyped on both sides of the homology arms for correct integration into the *EphB4* locus. The neomycin phosphotransferase selectable marker cassette, which was flanked by *frt* sites, was deleted after subsequent breeding to mice expressing flp recombinase under the CAG promoter.

For embryonic induction of Cre recombination, 4-hydroxytamoxifen (4-OHT, Sigma) was dissolved in peanut oil (10 mg/ml). 1 mg was administered to pregnant females by intraperitoneal injection at the indicated developmental stages. For induction during early postnatal development, mice were administered by intraperitoneal injection at P1 and P2 with 50 µg of 4-OHT dissolved in Ethanol. All strains were maintained and analysed on C57BL/6J background. Experimental procedures were approved by the United Kingdom Home Office and the Uppsala Laboratory Animal Ethical Committee.

Immunofluorescence. For whole-mount immunostaining, tissues were fixed in 4% paraformaldehyde (PFA) for 2h at RT followed by permeabilization in 0.3% Triton X-100 PBS (PBSTx) and blocking in PBSTx 3% milk. Primary antibodies were incubated at 4°C overnight in blocking buffer. After washing several times, the samples were incubated with fluorocrome-conjugated secondary antibodies in blocking buffer for 2 hours, before further washing and mounting in Mowiol. The following primary antibodies were used: goat anti-mouse EphB4 (AF446, R&D Systems), goat anti-human VE-Cadherin (sc-6458, Santa Cruz Biotechnology), rabbit anti-human Prox1 (generated against human Prox1 C-terminus (567-737aa)), rabbit anti-GFP (A11122, Invitrogen), chicken anti-GFP (Ab13970, Abcam), rat anti-PECAM-1 (553370, BD Pharmigen), rat anti-Endomucin (sc-65495, Santa Cruz) and rabbit anti-Lyve1 (103-PA50AG, Reliatech). Secondary antibodies conjugated to AF488, Cy3 or AF647 were obtained from Jackson ImmunoResearch. Controls were littermate embryos and mice of the following genotypes: *Ephb4$^{flox/+}$;R26-mTmG^{+};Prox1-CreER^{T2+}, Ephb4$^{flox/flox}$;R26-mTmG^{+};Prox1-CreER^{T2-} or Ephb4$^{flox/flox}$;R26-mTmG^{-};Prox1-CreER^{T2-}.*

For analysis of LVVs, 100µm coronal vibratome sections of E13.5 embryos were cut and stained as described above. Single plane images of the valve were taken where the valve was

clearly visible. Only valves that appeared intact were included in the classification. 5 control embryos (*Ephb4$^{flox/+}$;R26-mTmG^{+};Prox1-CreER^{T2+}* and *Ephb4$^{+/+}$;R26-mTmG^{+};Prox1-CreER^{T2+}*) were cut and 11 valves were imaged and included in the quantification. For mutant embryos (*Ephb4$^{flox/flox}$;R26-mTmG^{+};Prox1-CreER^{T2+}*) 13 valves from 9 embryos were imaged.

Image acquisition. Stereomicroscope images were acquired using a Leica MZ16F fluorescence microscope with a Leica DFC420C camera and Leica Microsystems software. Confocal images were acquired using Zeiss LSM 780 confocal microscope and Zen 2009 software, or Leica SP8 confocal microscope and Leica Application Suite X software. Figures 5C and 5D were acquired as 4x2 tile scans with a HCX PL APO CS 10x/0.40 DRY objective. Figure 6 was acquired using a Fluotar VISIR 25x/0.95 Water objective. Supplemental figure 4A was taken with a HC PL APO CS2 63x/1.30 GLYC objective; supplemental figure 4B (P6 mesentery) using a C-Aphochromat 40x/1.20 W Korr M27 objective and supplemental figures 4B (E18 mesentery), 4C and 4D were acquired using a Plan-Apochromat 20x/0.8 Ph2. All confocal images represent maximum intensity projections of z-stacks except images in Figure 6.

Lymphoscintigraphy. Lymphoscintigraphy is the imaging of the lymphatic system by injecting radioactive isotope (technetium-99m) into the web spaces between the toes and/or fingers and quantification of uptake into the inguinal lymph nodes for foot injections and axillary nodes for hand injection after 2 h with a gamma camera.

Statistical analysis. P values representing difference in proportion of edematous and non-edematous mutant versus control littermates (Figure 5B) and proportion of normal and abnormal LVVs (Figure 6D) were calculated using Chi square/Fisher's Exact (2-tailed). A P value less than 0.05 was considered significant.

Study approval. Subjects in this study were recruited through genetic and lymphovascular clinics in Norway and the United Kingdom. Ethical approval for this study was obtained from the Norwegian Regional Committees for Medical and Health Research Ethics, West (REC ref: 2011/2453) and the South West London Research Ethics Committee (REC Ref: 05/Q0803/257). Written informed consent was obtained for all subjects. All affected individuals and family members underwent a detailed physical examination. Animal study was approved by the United Kingdom Home Office and the Uppsala Laboratory Animal Ethical Committee.

Author contributions

Designing research study: SMA, IMC, SB, SJ, TM, PO

Conducting experiments: SMA, IMC, EF, RH, AV, SL, HJ, CK

Providing NGS pipeline: MAS, KP, SL, CG, AH

Analysing data: SMA, IMC, RH, AV, SL, SB, SJ, SM, TM, PO

Providing reagents, material, patients: GA, GB, KG, MW, JW, SB, PSM, SGR, SM, TM, PO

Writing the manuscript: SMA, IMC, SB, SJ, SM, TM, PO

Supervised the research: PSM, SGR, SJ, SM, MPS, TM, PO

Acknowledgements

We extend our thanks to the patients and their families. This work was supported by the British Heart Foundation to SMA/IMC (SP/13/5/30288), KG (FS/11/40/28739), CK (FS/15/39/31526) and PO (PG/10/58/28477); the Newlife Foundation for Disabled Children to EF (12-13/01); the National Institute for Health Research (NIHR) Biomedical Research Centre based at Guy's and St Thomas' NHS Foundation Trust and King's College London to MAS; the National Institutes of Health (NIH) to SL (Fellowship Grants F32HL110473 and K99HL119617); the Swedish Cancer Foundation and the Swedish Research Council to TM; Cancer Research UK to AV/TM.

References – need moving to here

1. Bellini C, et al. Etiology of Non-Immune Hydrops Fetalis: An Update. *Am J Med Genet A.* 2015;167A(5):1082-1088.
2. Connell FC, et al. The classification and diagnostic algorithm for primary lymphatic dysplasia: an update from 2010 to include molecular findings. *Clin Genet.* 2013;84(4):303-314.
3. Alders M, et al. Mutations in CCBE1 cause generalized lymph vessel dysplasia in humans. *Nat Genet.* 2009;41(12):1272-1274.
4. Connell F, et al. Linkage and sequence analysis indicate that CCBE1 is mutated in recessively inherited generalised lymphatic dysplasia. *Hum Genet.* 2010;127(2):231-241.
5. Alders M, et al. Hennekam syndrome can be caused by FAT4 mutations and be allelic to Van Maldergem syndrome. *Hum Genet.* 2014;133(9):1161-1167.
6. Fotiou E, et al. Novel mutations in PIEZO1 cause an autosomal recessive generalized lymphatic dysplasia with non-immune hydrops fetalis. *Nat Commun.* 2015;6:8085.
7. Kuijper S, et al. Regulation of angiogenesis by Eph-Ephrin interactions. *Trends Cardiovasc Med.* 2007;17(5):145-151.
8. Pitulescu ME, Adams RH. Eph/ephrin molecules-a hub for signaling and endocytosis. *Genes Dev.* 2010;24(22):2480-2492.
9. Wang HU, et al. Molecular distinction and angiogenic interaction between embryonic arteries and veins revealed by ephrin-B2 and its receptor Eph-B4. *Cell.* 1998;93(5):741-753.
10. Adams RH, et al. Roles of ephrinB ligands and EphB receptors in cardiovascular development: demarcation of arterial/venous domains, vascular morphogenesis, and sprouting angiogenesis. *Genes Dev.* 1999;13(3):295-306.
11. Zhang G, et al. EphB4 forward signalling regulates lymphatic valve development. *Nat Commun.* 2015;6:6625.
12. Makinen T, et al. PDZ interaction site in ephrinB2 is required for the remodeling of lymphatic vasculature. *Genes Dev.* 2005;19(3):397-410.
13. Martinez-Corral I, et al. Nonvenous origin of dermal lymphatic vasculature. *Circ Res.* 2015;116(10):1649-1654.
14. Srinivasan RS, Oliver G. Prox1 dosage controls the number of lymphatic endothelial cell progenitors and the formation of the lymphovenous valves. *Genes Dev.* 2011;25(20):2187-2197.
15. Hagerling R, et al. A novel multistep mechanism for initial lymphangiogenesis in mouse embryos based on ultramicroscopy. *EMBO J.* 2013;32(5):629-644.
16. Geng X, et al. Multiple mouse models of primary lymphedema exhibit distinct defects in lymphovenous valve development. *Dev Biol.* 2016;409(1):218-233.
17. Bazigou E, et al. Genes regulating lymphangiogenesis control venous valve formation and maintenance in mice. *J Clin Invest.* 2011;121(8):2984-2992.
18. Chennakesava CS, et al. Differential expression of the receptor tyrosine kinase EphB4 and its ligand Ephrin-B2 during human placental development. *Placenta.* 2006;27(9-10):959-967.
19. Red-Horse K, et al. EPHB4 regulates chemokine-evoked trophoblast responses: a mechanism for incorporating the human placenta into the maternal circulation. *Development.* 2005;132(18):4097-4106.
20. Turner CJ, et al. Integrin-alpha 5 beta 1 is not required for mural cell functions during development of blood vessels but is required for lymphatic-blood vessel separation and lymphovenous valve formation. *Dev Biol.* 2014;392(2):381-392.
21. Hess PR, et al. Platelets mediate lymphovenous hemostasis to maintain blood-lymphatic separation throughout life. *J Clin Invest.* 2014;124(1):273-284.
22. Bazigou E, et al. Integrin-alpha 9 Is Required for Fibronectin Matrix Assembly during Lymphatic Valve Morphogenesis. *Dev Cell.* 2009;17(2):175-186.

23. Sabine A, et al. Mechanotransduction, PROX1, and FOXC2 Cooperate to Control Connexin37 and Calcineurin during Lymphatic-Valve Formation. *Dev Cell.* 2012;22(2):430-445.
24. Kazenwadel J, et al. GATA2 is required for lymphatic vessel valve development and maintenance. *J Clin Invest.* 2015;125(8):2979-2994.
25. Brice G, et al. Analysis of the phenotypic abnormalities in lymphoedema-distichiasis syndrome in 74 patients with FOXC2 mutations or linkage to 16q24. *J Med Genet.* 2002;39(7):478-483.
26. Mellor RH, et al. Mutations in FOXC2 are strongly associated with primary valve failure in veins of the lower limb. *Circulation.* 2007;115(14):1912-1920.
27. Karkkainen MJ, et al. Missense mutations interfere with VEGFR-3 signalling in primary lymphoedema. *Nat Genet.* 2000;25(2):153-159.
28. Seiradake E, et al. Structurally encoded intraclass differences in EphA clusters drive distinct cell responses. *Nat Struct Mol Biol.* 2013;20(8):958-964.
29. Schaupp A, et al. The composition of EphB2 clusters determines the strength in the cellular repulsion response. *J Cell Biol*. 2014:409-422.
30. Zimmer M, et al. EphB-ephrinB bi-directional endocytosis terminates adhesion allowing contact mediated repulsion. *Nat Cell Biol.* 2003;5(10):869-878.
31. Quinlan AR, Hall IM. BEDTools: a flexible suite of utilities for comparing genomic features. *Bioinformatics.* 2010;26(6):841-842.
32. Li H, et al. The Sequence Alignment/Map format and SAMtools. *Bioinformatics.* 2009;25(16):2078-2079.
33. Simpson MA, et al. Mutations in NOTCH2 cause Hajdu-Cheney syndrome, a disorder of severe and progressive bone loss. *Nat Genet.* 2011;43(4):303-305.
34. Wang K, et al. ANNOVAR: functional annotation of genetic variants from high-throughput sequencing data. *Nucleic Acids Res.* 2010;38(16):e164.
35. Rozen S, Skaletsky H. Primer3 on the WWW for general users and for biologist programmers. *Methods Mol Biol.* 2000;132:365-386.
36. Muzumdar MD, et al. A global double-fluorescent Cre reporter mouse. *Genesis.* 2007;45(9):593-605.
37. Datsenko KA, Wanner BL. One-step inactivation of chromosomal genes in Escherichia coli K-12 using PCR products. *Proc Natl Acad Sci U S A.* 2000;97(12):6640-6645.

Figures and figure legends

Figure 1. Mutations in *EPHB4* cause Lymphatic-Related Hydrops Fetalis (LRHF)

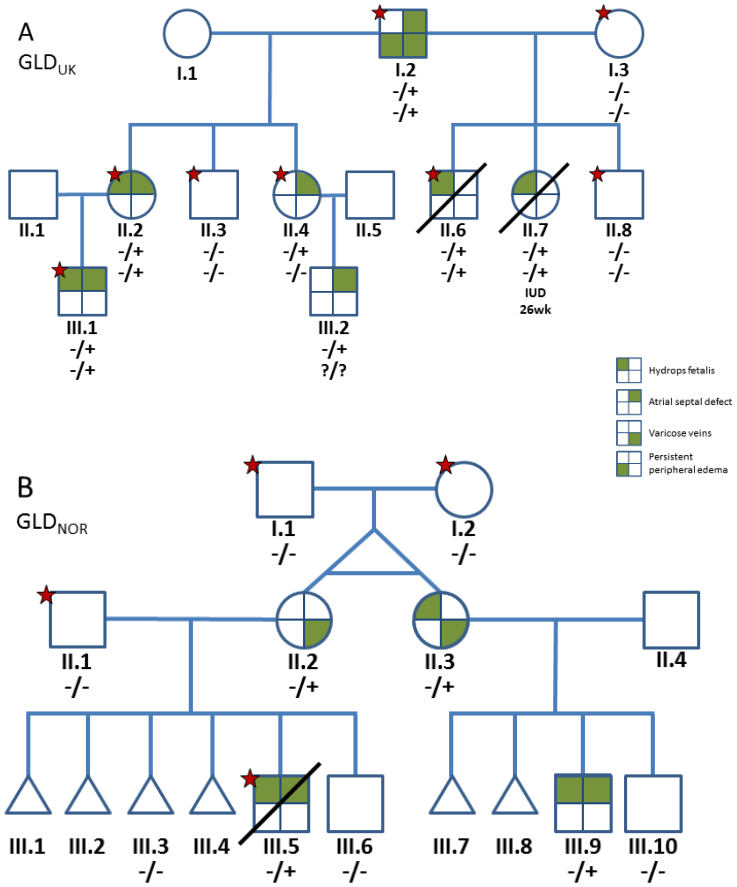

(A) Pedigree of UK GLD family, **(B)** pedigree of Norwegian GLD family. Stars indicate which samples have been exome sequenced. Genotypes indicated by hyphen (-) is the wildtype allele and a plus (+) the mutant allele. Top row of genotypes in GLD$_{UK}$ genogram is for *EPHB4* and bottom row of genotypes is *MIER2*. Triangles, first trimester miscarriages; IUD, intra-uterine death. GLD$_{NOR}$:III.3 had trisomy 18.

Figure 2. Imaging of the lymphatic system in LRHF

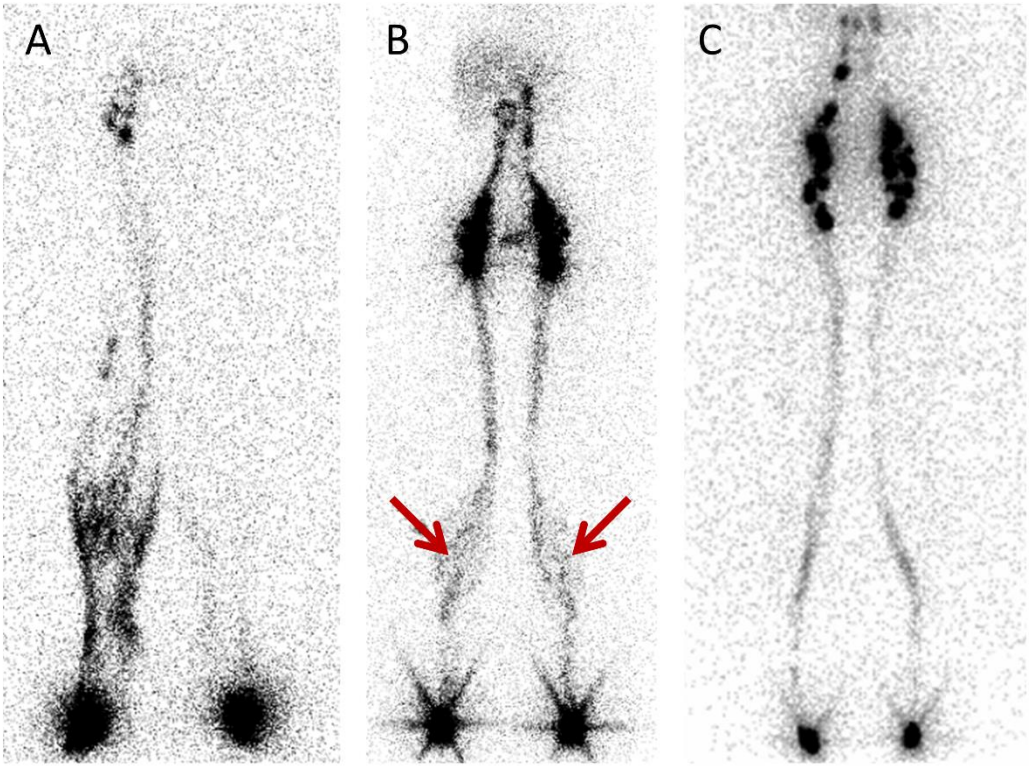

Anterior view lower limb lymphoscintigraphy 2 h after injection with radionuclide. **(A)** GLD$_{UK}$I.2, rerouting through skin and superficial tissues in the right leg and markedly reduced transport in the left leg. **(B)** GLD$_{UK}$II.4, normal uptake of tracer in the lymph nodes in the groin area, but with some rerouting in the calves (seen as the dark shading; arrows). **(C)** Unaffected subject with symmetrical transport of radionuclide within collecting lymph vessels in the leg.

Figure 3. Effect of p.Arg739Glu and p.Ile782Ser mutations on EPHB4 tyrosine phosphorylation in HEK293T cells

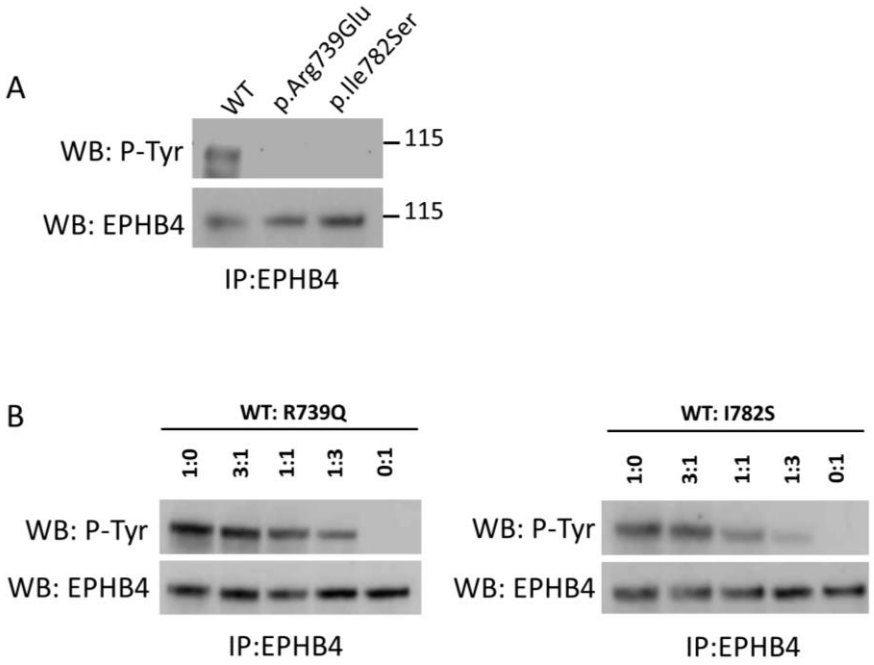

(A) HEK293T cells were transfected with expression plasmids for EPHB4 WT and p.Arg739Glu and p.Ile782Ser mutants. Receptor phosphorylation was analysed by immunoprecipitation and western blotting using anti-phosphotyrosine (P-Tyr, upper part) and EPHB4 (lower part) antibodies. The position of molecular mass markers (in kDa) is indicated to the right of the gel. **(B)** EPHB4 WT and p.Arg739Glu and p.Ile782Ser mutants were cotransfected into HEK293T cells in different ratios of WT to mutant plasmid. Receptor phosphorylation was analysed as above. One representative experiment (n=3) is shown.

Figure 4. Effect of p.Arg739Glu and p.Ile782Ser mutations on EPHB4 tyrosine phosphorylation in LECs after EphrinB2 stimulation

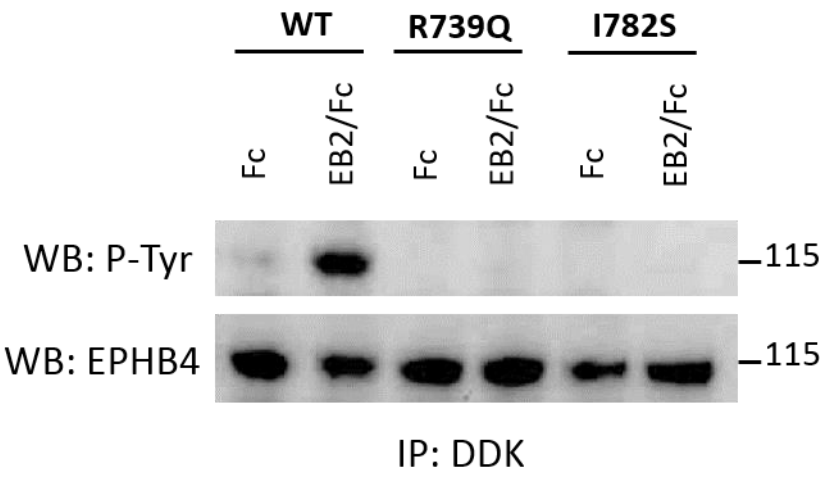

LECs were transfected with expression plasmids for Myc-DDK-tagged EPHB4 WT and p.Arg739Glu and p.Ile782Ser mutants. The cells were stimulated with 1µg/ml clustered EphrinB2/Fc (EB2/Fc) or Fc alone. Receptor phosphorylation was analysed by immunoprecipitation with anti-DDK antibody and western blotting using anti-phosphotyrosine (P-Tyr, upper part) and EPHB4 (lower part) antibodies. The position of molecular mass markers (in kDa) is indicated to the right of the gel. One representative experiment (n=2) is shown.

Figure 5. Early embryonic deletion of *Ephb4* leads to subcutaneous edema and abnormal dermal lymphatic vasculature

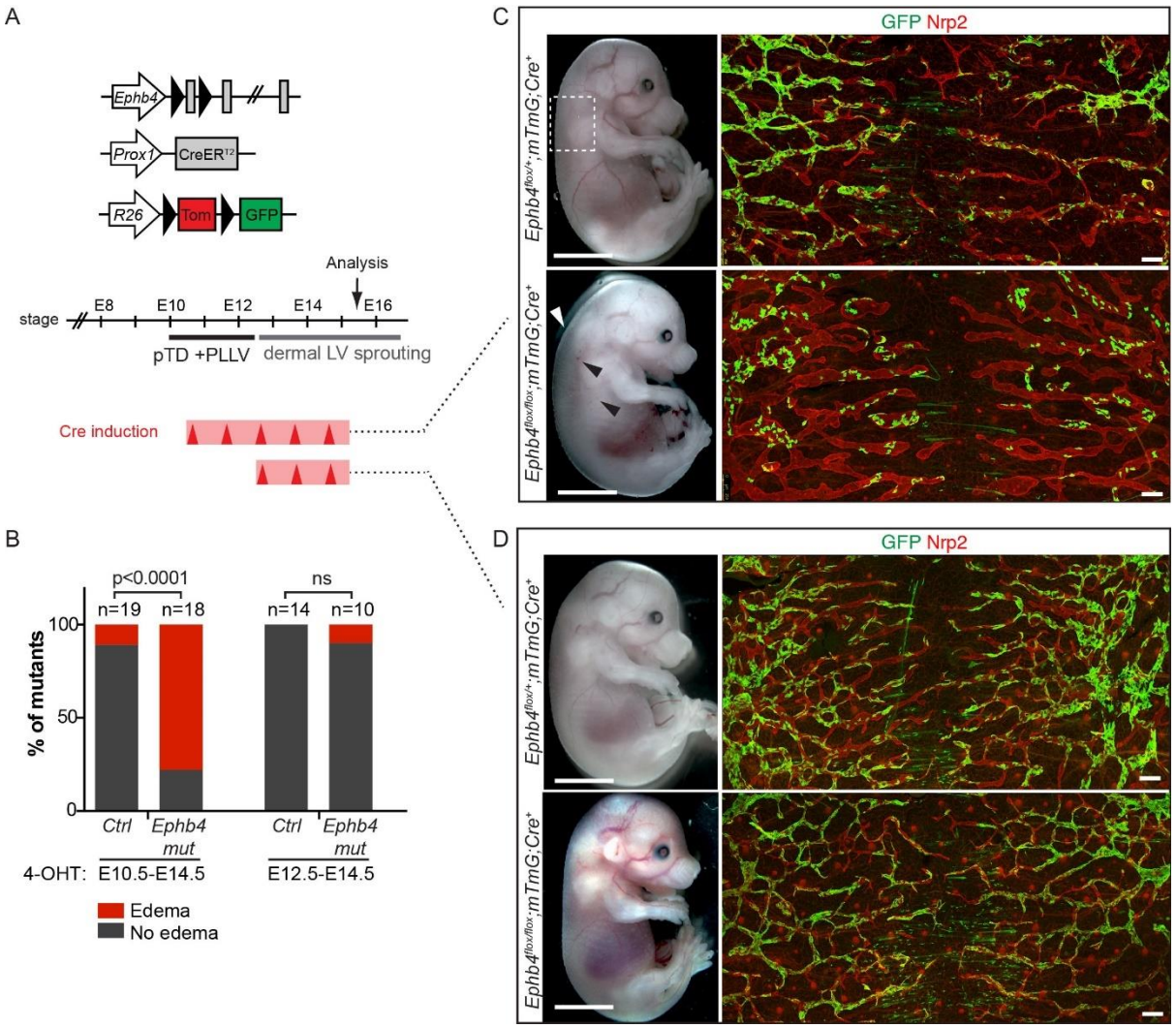

(A) Schematic of the transgenes and 4-OHT administration (Cre induction; red arrowheads) schedule used for *Ephb4* deletion in the lymphatic vasculature. Timing of primitive lymphatic vessel (pTD = primordial thoracic duct, PLLV = peripheral longitudinal lymphatic vessel, LV = lymphatic vessel) formation and time-point for analysis are indicated. **(B)** Edema in E15.5 control and *Ephb4* mutant embryos after different 4-OHT treatments. P values Fisher's Exact test; ns = not significant. **(C, D)** Left panels: E15.5 $Ephb4^{flox/+}$ and $Ephb4^{flox/flox}$*;R26-mTmG; Prox1-CreER*^{T2} embryos. Most mutants treated with 4-OHT at E10.5-

E14.5 showed subcutaneous edema (white arrowhead) and blood-filled lymphatic vessels (black arrowheads). Boxed area indicates the area of the skin imaged on the right. Right panels: Whole-mount immunofluorescence of E15.5 thoracic skin for Nrp2 (red) and GFP (green) to stain lymphatic vessels and gene targeted cells, respectively. Scale bars: 200 µm (C and D).

Figure 6. Early embryonic deletion of *Ephb4* leads to a failure of lymphovenous valve formation

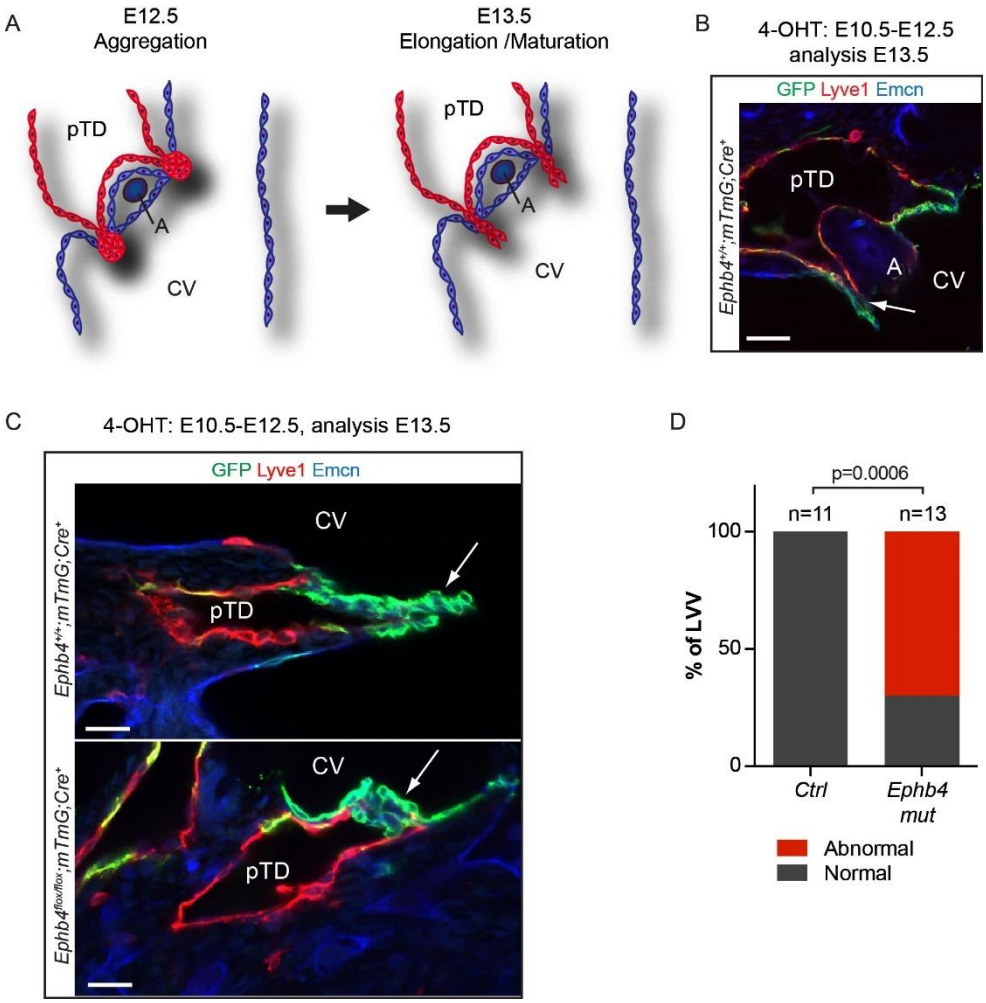

(A) Schematic representation of lymphovenous valve (LVV) formation (adapted from Geng et al. (16)). pTD, primordial thoracic duct; CV, cardinal vein; A, artery. **(B)** Whole-mount immunofluorescence of a transverse section of E13.5 *Ephb4*$^{+/+}$*;R26-mTmG;Prox1-CreER*^{T2} embryo for indicated proteins. GFP shows efficient Cre-mediated recombination in the LVV that extends to the lumen of the CV (arrow). **(C)** Whole-mount immunofluorescence of E13.5 LVVs showing extension of the valve leaflets to the lumen of CV (arrow) in control (upper panel, n=11 out of 11) but not in *Ephb4* mutant embryo (lower panel, n=9 out of 13).

(D) Quantification of LVV morphology in control and *Ephb4* mutant embryos. Normal, elongated leaflets; abnormal, no leaflets. P value Fisher's Exact test. Scale bars: 50 µm (B), 25 µm (C).

Table 1. Clinical features of family members carrying *EPHB4* mutations.

Family	GLD_{NOR}				GLD_{UK}						
Id	II.2[A]	II.3[A]	III.5	III.9	I.2	II.2	II.4	II.6	II.7	III.1	III.2
Gender	F	F	M	M	M	F	F	M	F	M	M
Age at last follow-up	37	37	na	6	55	30	24	na	na	8	4
NT @ 11/12 wk in mm (normal <3mm)	\	\	2.1	1.8	\	\	\	3	3.8	2.8	\
Fetal hydrops diagnosed (weeks)	\	\	28	28	-	+	-	20	20	22	-
Extent of hydrops	\	\	PE, SC, TCx3	PE, As, SC, TCx4	na	PE, As, SC	na	PE, As, SC, PC	PE, As, SC	PE,SC	na
Gestation at birth (weeks)	34	34	30	30	36	34	38	34	IUD 26	32	40
Systemic involvement	An	RD, CT, An	CT	CT, An	-	CT, As	-	CT, As	na	CT	-
Peripheral swelling at birth	BL, RA	T, Fa	+	+	-	+	-	+	na	-	-
Spontaneous resolution of all swellings	+	+	ND 1.5 days	+	na	+	na	ND 21 days	na	+	na
Atrial septal defect (ASD)	-	-	+	+	+	+	smallASD/PFO	-	-	+	multiple ASDs
Persistent peripheral edema	-	-	na	-	BL at 15y	-	-	na	na	-	-
Varicose veins	+	+	na	-	+	-	-	na	na	\	\

[A]monozygotic twins; As, ascites; An, anemia; BL, bilateral lower limb; CT, chylothoraces; Fa, facial edema; F, female; IUD, intra-uterine death; M, male; ND, neonatal death; NT, nuchal translucency scan; PC, pericardial effusions; PE, pleural effusions; PFO, Patent Foramen Ovale; RA,

right arm edema; RD, respiratory distress; SC, subcutaneous edema; T, Truncal; TC, thoracocentesis in utero; \ not recorded; na, not applicable;

-, no; +, yes.